AIAA JOURNAL
Vol. 35, No. 8, August 1997

Mixed Laminate Theory and Finite Element for Smart Piezoelectric Composite Shell Structures

Dimitris A. Saravanos*
Ohio Aerospace Institute, Cleveland, Ohio 44142

Mechanics for the analysis of laminated composite shells with piezoelectric actuators and sensors are presented. A new mixed laminate theory for piezoelectric shells is developed in curvilinear coordinates that combines single-layer assumptions for the displacements and a layerwise representation for the electric potential. The resultant coupled governing equations for curvilinear piezoelectric laminates are described. Structural mechanics are subsequently developed and an eight-node finite element is formulated for the static and dynamic analysis of adaptive composite shell structures of general laminations containing piezoelectric layers. Evaluations of the method and comparisons with reported results were performed. Numerical results for cylindrical laminated piezoelectric composite panels with continuous piezoceramic actuators and cantilever shells with continuous or discrete piezoelectric actuators and sensors illustrate the advantages of the method and quantify the effects of curvature on the electromechanical response of piezoelectric shells.

I. Introduction

SMART composite laminates and adaptive composite structures with embedded piezoelectric sensors and actuators seem to combine some of the superior mechanical properties of composites with the additional capabilities to sense deformations and stress states and to adapt their response accordingly. Such novel materials and structures have received substantial research attention. Adaptive curvilinear composite shells with embedded piezoelectric devices are among the structural configurations of most practical interest because curvilinear structural configurations are commonly used in aeronautical, aerospace, automotive, and other engineering applications. Yet, smart shell structures are also among the more challenging to study both analytically and experimentally, and their analysis remains an active research area. Consequently, the present paper presents theoretical foundations and mechanics for the coupled analysis of curvilinear piezoelectric laminates and shell structures.

Numerous theories and models have been proposed for the analysis of laminated composite beams and plates containing active and passive piezoelectric layers. Simplified approaches attempting to replicate the induced strains and electric fields generated by a piezoelectric layer under an external electric field have been proposed.[1–5] Variational methods and finite element models for piezoelectric solids have also been reported by Allik and Hughes,[6] Naillon et al.,[7] Tzou and Tseng,[8] and Ha et al.[9] Layerwise theories were reported for infinite piezoelectric plates by Pauley[10] and for finite elastic laminated beams and plates with induced strain actuation by Robbins and Reddy.[11,12] Coupled layerwise theories and finite elements for laminated composite beams and plates with piezoelectric actuators and sensors were also developed by Heyliger et al.,[13] Saravanos and Heyliger,[14] and Saravanos et al.,[15] which consider the complete electromechanical response of smart piezoelectric plate structures under external mechanical or electrical loading. An exact piezoelasticity solution has been also reported by Heyliger and Saravanos[16] for piezoelectric laminated plates.

Analytical formulations have been proposed for laminated piezoelectric shells. Dökmeci[17] has reported theoretical work for the vibration of single-layered piezoelectric shells. Lammering[18] developed a Reissner–Middlin type shear deformable finite element for shells with surface bonded piezoelectric layers. Koconis et al.[19] have reported a Ritz method for sandwich composite shells with embedded piezoelectric actuators. Tzou and Garde[20] reported approaches for the analysis of thin laminated shells based on Kirchhoff–Love assumptions. Theoretical formulations that include Reissner–Middlin type of shear deformation theory and rotary inertia effects were presented for curved beams and rings by Larson and Vinson[21] and for shells by Tzou and Zhong.[22] The previous approaches effectively utilize equivalent force/moment representations of the induced piezoelectric strain by attempting to replicate the electric fields in the piezoelectric layers and do not solve the coupled equations of piezoelectricity directly. This limitation typically results in inferior solutions for smart structures with embedded piezoceramic sensors, including the prediction of sensory electric signals. Alternatively, Tzou and Ye[23] proposed the analysis of piezoelectric shells as a layerwise assembly of curvilinear solid piezoelectric triangular elements, and Heyliger et al.[24] developed discrete-layer mechanics and a finite element for laminated piezoelectric solids. These are effectively three-dimensional approaches, and although they are very powerful computationally, they typically result in large problem sizes and high computational effort.

It seems, therefore, that a coupled piezoelectric shell theory that can accurately and efficiently predict the electromechanical response of thin and intermediately thick piezoelectric-composite shells has not been reported yet. Consequently, this paper attempts to remedy this void in current technology and presents the theoretical foundations of a new coupled piezoelectric shell theory and, more importantly, the development and evaluation of a corresponding finite element formulation that enables the formal analysis of piezoelectric composite shells. The mechanics are truly coupled; that is, they involve approximate through-the-thickness fields for both displacements and electric potential and solve the coupled equations of piezoelectricity in curvilinear coordinates. Moreover, the proposed laminate shell theory is unique because it utilizes different types of approximations for the displacement and electric potential, that is, first-order shear theory type of assumptions for the displacements and the so-called discrete-layer (or layerwise) approximation for the electric potential.[14,15] The combination of mixed through-the-thickness approximations for the displacement and electric potential is a unique feature of the mechanics that is termed, hereafter, as mixed piezoelectric shell theory (MPST), which enables the analysis of thin and moderately thick piezoelectric shells of general laminations with reasonable computational efficiency, while maintaining sufficient detail in the approximation of the electrical fields. The approach is particularly suitable for finite element formulations, as it ensures direct calculation and continuity of the sensory electric potential over the shell structure, thus avoiding the drawbacks of uncoupled approaches that effectively back calculate the sensory voltage from mechanical strains. These drawbacks may become more severe at low thicknesses due to overstiffening associated with shear theory. Finite element formulations are also presented, based

Received March 6, 1996; revision received April 11, 1997; accepted for publication May 9, 1997.

*Senior Research Associate, 22800 Cedar Point Road; currently Assistant Professor, Department of Mechanical Engineering and Aeronautics, University of Patras, Patras 26500, Greece. Member AIAA.

on MPST, and an eight-node curvilinear shell element is developed for the numerical analysis of piezoelectric composite shells.

II. Piezoelectric Laminated Shells

This section describes the analytical formulation for curvilinear laminates with embedded sensory and active piezoelectric layers. The curvilinear laminate configuration is shown schematically in Fig. 1. Each ply of the laminate remains parallel to a reference curvilinear surface A_0. An orthogonal curvilinear coordinate system $O\xi\eta\zeta$ is defined, such that the axes ξ and η lie on the curvilinear reference surface A_0, whereas the axis ζ remains straight and perpendicular to the layers of the laminate. A global Cartesian coordinate system $Oxyz$ is used to define A_0, hence, a point $r = (x, y, z)$ on the curvilinear laminate is

$$r(\xi, \eta, \zeta) = r_0(\xi, \eta) + \zeta\hat{\zeta} \tag{1}$$

where $r_0 = (x_0, y_0, z_0)$ are the Cartesian coordinates of the reference surface A_0, and $\hat{\zeta}$ indicates the unit vector perpendicular to the reference surface.

Governing Material Equations

Each ply is assumed to consist of a linear piezoelectric material with properties defined on the orthogonal curvilinear system $O\xi\eta\zeta$ and constitutive equations of the following form[25]:

$$\sigma_i = C_{ij}^E S_j - e_{ik} E_k, \qquad D_l = e_{lj} S_j + \varepsilon_{lk}^S E_k \tag{2}$$

where $i, j = 1, \ldots, 6$ and $k, l = 1, \ldots, 3$; σ_i and S_i are the mechanical stresses and engineering strains in vectorial notation; E_k is the electric field vector; D_l is the electric displacement vector; C_{ij} is the elastic compliance and stiffness tensors; e_{lj} is the piezoelectric tensor; and ε_{lk} is the electric permittivity tensor of the material. Superscripts E and S indicate constant electric field and strain conditions, respectively. The axes 1, 2, and 3 of the material are parallel to the curvilinear axes ξ, η, and ζ, respectively. The materials are assumed to be monoclinic class 2 crystals with a diad axis parallel to the ζ axis. The assumed material class is general enough such that Eqs. (2) may encompass the behavior of off-axis homogenized piezoelectric plies as well as passive composite plies.

The tensorial strain S_{ij} and electric field components in a curvilinear coordinate system are related to the displacements and electric potential, respectively.[26] For the curvilinear system $O\xi\eta\zeta$ defined in Fig. 1, the strain-displacement relationships are given in Refs. 27 and 28, while the relation of the electric field vector E_k to the electric potential ϕ is provided in Refs. 22 and 28.

Mixed Field Laminate Theory

A new theory for piezoelectric laminates is proposed that combines linear displacement fields through the thickness of the laminate for the displacements u and v (along the ξ and η axes, respectively) with a layerwise electric potential field through the laminate, consisting of N discrete continuous segments (Fig. 2). Previous work by Saravanos and Heyliger[14] and Saravanos et al.[15] on layerwise theories for piezoelectric beams and plates has demonstrated the advantages and necessity of layerwise approaches in capturing the complicated electric fields and interactions that are present in piezoelectric actuators and sensors. Consequently, by mixing a layerwise electric potential field with first-order shear theory assumptions for the displacements, a new piezoelectric shell laminate

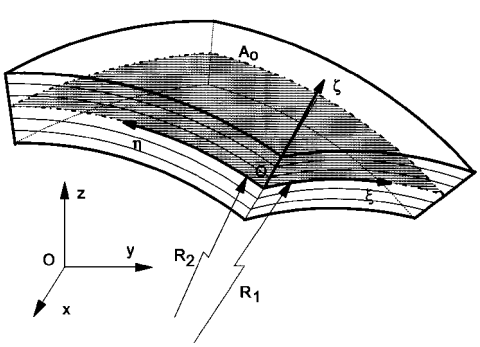

Fig. 1 Curvilinear piezoelectric laminate and coordinate systems.

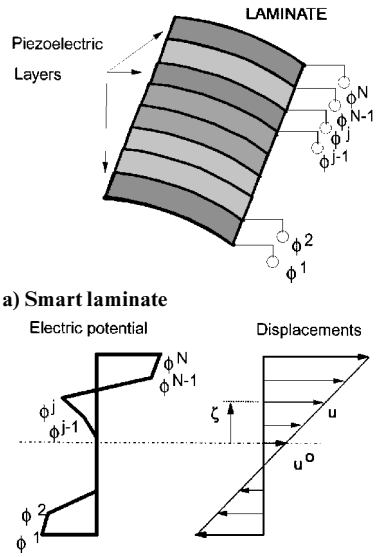

Fig. 2 Typical piezoelectric laminate configuration: a) concept and b) assumed through-the-thickness displacement and electric potential fields.

theory (MPST) is postulated, which can 1) accurately and efficiently model thin and/or moderately thick laminated piezoelectric shells with arbitrary laminations and electric configurations and 2) capture the through-the-thickness electric heterogeneity induced by the embedded piezoelectric sensors and actuators.

The discrete-layer assumption effectively subdivides the laminate into $N - 1$ sublaminates (or discrete layers). The subdivision can be arbitrarily controlled according to the configuration of the piezoelectric layers and/or the required detail of approximation. A continuous electric potential is assumed in each sublaminate, such that a C_0 continuous variation results through the thickness of the laminate (see Fig. 2). The displacements and electric potential of the mixed-field theory take the following form:

$$\begin{aligned} u(\xi, \eta, \zeta, t) &= u^0(\xi, \eta, t) + \zeta\beta_\xi(\xi, \eta, t) \\ v(\xi, \eta, \zeta, t) &= v^0(\xi, \eta, t) + \zeta\beta_\eta(\xi, \eta, t) \\ w(\xi, \eta, \zeta, t) &= w^0(\xi, \eta, t) \\ \phi(\xi, \eta, \zeta, t) &= \sum_j^N \phi^j(\xi, \eta, t)\Psi^j(\zeta) \end{aligned} \tag{3}$$

where u^0, v^0, and w^0 are displacements along the ξ, η, and ζ axes, respectively, on the reference surface A_0; superscript j indicates the points ζ^j at the beginning and end of each discrete layer; ϕ^j is the electric potential at each point ζ^j (see Fig. 2); $\Psi^j(z)$ are interpolation functions; and β_ξ and β_η are the rotation angles defined as

$$\beta_\xi = -(w^0_{,\xi}/g^0_{11}) + (u^0/R_1), \qquad \beta_\eta = -(w^0_{,\eta}/g^0_{22}) + (v^0/R_2) \tag{4}$$

where R_i are the local radii of curvature (Fig. 1). Two unique advantages of the laminate theory are obvious: 1) the complete electromechanical state of the smart laminate is represented and 2) the formulation entails the inherent option to select the detail of approximation of the electric field. Linear interpolation functions $\Psi(z)$ were considered in this paper.

The Love assumption is further implemented; that is, the local radii of the shell are substantially higher than the thickness ($h/R_i \ll 1$), yielding ($1 + \zeta/R_i \approx 1$). The Love assumption is appropriate for shallow shells, yet additional work will be presented in the near future for deep shells with the Love assumption removed. Now, in the context of Eqs. (3), the engineering strains become

$$\begin{aligned} S_i(\xi, \eta, \zeta, t) &= S_i^0(\xi, \eta, t) + \zeta k_i(\xi, \eta, t), \qquad i = 1, 2, 6 \\ S_3(\xi, \eta, \zeta, t) &= 0 \\ S_i(\xi, \eta, \zeta, t) &= S_i^0(\xi, \eta, t), \qquad i = 4, 5 \end{aligned} \tag{5}$$

where S^0 and k are the strain and curvatures at the reference surface, defined as follows:

$$S_1^0 = \frac{1}{g_{11}^0}\left(u^0_{,\xi} + \frac{g^0_{11,\eta}}{g^0_{22}}v^0\right) + \frac{w^0}{R_1}, \qquad S_2^0 = \frac{1}{g_{22}^0}\left(v^0_{,\eta} + \frac{g^0_{22,\xi}}{g^0_{11}}u^0\right) + \frac{w^0}{R_2}$$

$$S_6^0 = \frac{1}{g_{11}^0}\left(v^0_{,\xi} - \frac{g^0_{11,\eta}}{g_{22}}u^0\right) + \frac{1}{g_{22}^0}\left(u^0_{,\eta} - \frac{g^0_{22,\xi}}{g_{11}}v^0\right) \tag{6}$$

$$S_4^0 = \beta_\eta + \frac{w^0_{,\eta}}{g^0_{22}} - \frac{v^0}{R_2}, \qquad S_5^0 = \beta_\xi + \frac{w^0_{,\xi}}{g^0_{11}} - \frac{u^0}{R_1}$$

$$k_1 = \frac{1}{g_{11}^0}\left(\beta_{\xi,\xi} + \frac{g^0_{11,\eta}}{g^0_{22}}\beta_\eta\right), \qquad k_2 = \frac{1}{g_{22}^0}\left(\beta_{\eta,\eta} + \frac{g^0_{22,\xi}}{g^0_{11}}\beta_\xi\right) \tag{7}$$

$$k_6 = \frac{1}{g_{11}^0}\left(\beta_{\eta,\xi} - \frac{g^0_{11,\eta}}{g^0_{22}}\beta_\xi\right) + \frac{1}{g_{22}^0}\left(\beta_{\xi,\eta} - \frac{g^0_{22,\xi}}{g^0_{11}}\beta_\eta\right)$$

where R_i are the local radii of curvature and g^0_{11} and g^0_{22} are the components of the metric tensor on the surface $A_0(\zeta = 0)$ defined as $g^0_{11} = \sqrt{(x^2_{0,\xi} + y^2_{0,\xi} + z^2_{0,\xi})}$ and $g^0_{22} = \sqrt{(x^2_{0,\eta} + y^2_{0,\eta} + z^2_{0,\eta})}$. The electric field vector also becomes

$$E_i(\xi, \eta, \zeta, t) = \sum_{j=1}^{N} E_i^j(\xi, \eta, t)\Psi^j(\zeta), \qquad i = 1, 2$$

$$E_3(\xi, \eta, \zeta, t) = \sum_{j=1}^{N} E_3^j(\xi, \eta, t)\Psi^j_{,\zeta}(\zeta) \tag{8}$$

where $\{E^j\}$ is the generalized electric field vector defined as

$$E_1^j = -(\Phi^j_{,\xi}/g^0_{11}), \qquad E_2^j = -(\Phi^j_{,\eta}/g^0_{22}), \qquad E_3^j = -\Phi^j \tag{9}$$

Equations of Motion

Considering that the Jacobian matrix $[J]$ of the transformation between the global Cartesian and curvilinear system $\bar{O}\xi\eta\zeta$ takes the form

$$|J| = \left|\frac{\partial(x, y, z)}{\partial(\xi, \eta, \zeta)}\right| = g^0_{11}g^0_{22}(1 + \zeta/R_1)(1 + \zeta/R_2) \approx g^0_{11}g^0_{22} \tag{10}$$

it is possible to rearrange the variational statement of the equations of motion and separate the through-the-thickness integration, as follows:

$$\int_{A_0} -[\delta H_L(S, E) - \delta T_L]\,\mathrm{d}\xi\,\mathrm{d}\eta + \oint_\Gamma (\delta u_i^T \bar{\tau}_i + \delta\phi\bar{D})\,\mathrm{d}\Gamma = 0 \tag{11}$$

where A_0 is the curvilinear reference surface; $\bar{\tau}$ and $\bar{D}$ are, respectively, the surface tractions and electric displacement on the boundary surface Γ; δH_L and δT_L are the variations of the electric enthalpy and kinetic energy of the laminate, defined as

$$\langle \delta H_L, \delta T_L \rangle = \int_0^h \langle \delta H, \delta T \rangle g^0_{11}g^0_{22}\,\mathrm{d}\zeta \tag{12}$$

and h is the laminate thickness. By combining Eqs. (5), (8), and (12) and integrating through the thickness, the variation of the electric enthalpy of the piezoelectric laminate is obtained as a quadratic expression of the generalized strain/electric field and the generalized laminate matrices,

$$\delta H_L = \delta S_i^0 A_{ij} S_j^0 + \delta S_i^0 B_{ij} k_j + \delta k_j B_{ji} S_i^0 + \delta k_i D_{ij} k_j$$
$$- \sum_{m=1}^{N} (\delta S_i^0 \bar{E}^m_{ik} E_k^m + \delta E_k^m \bar{E}^m_{ki} S_i^0 + \delta k_j \hat{E}_j^m E_3^m + \delta E_3^m \hat{E}_j^m k_j)$$
$$- \sum_{m=1}^{N}\sum_{n=1}^{N} \delta E_k^m G^{mn}_{kl} E_l^m \tag{13}$$

In the preceding equation, $[A]$, $[B]$, and $[D]$ are the stiffness matrices of the curvilinear laminate,

$$\langle A_{ij}, B_{ij}, D_{ij} \rangle = g^0_{11}g^0_{22} \sum_{L} \int_{\zeta}^{\zeta_{+1}} C_{ij}\langle 1, \zeta, \zeta^2 \rangle \mathrm{d}\zeta \qquad i, j = 1, 2, 6 \tag{14}$$

$$A_{ij} = g^0_{11}g^0_{22} \sum_{L} \int_{\zeta}^{\zeta_{+1}} C_{ij}\,\mathrm{d}\zeta, \qquad i, j = 4, 5$$

$[\bar{E}^m]$ and $[\hat{E}^m]$ are the piezoelectric matrices,

$$\langle \bar{E}^m_{ij}, \hat{E}^m_{ij} \rangle = g^0_{11}g^0_{22} \sum_{L} \int_{\zeta}^{\zeta_{+1}} e_{ij}\Psi^m_{,\zeta}(\zeta)\langle 1, \zeta \rangle \mathrm{d}\zeta \qquad i = 3, \quad j = 1, 2, 6 \tag{15}$$

$$\bar{E}^m_{ij} = g^0_{11}g^0_{22} \sum_{L} \int_{\zeta}^{\zeta_{+1}} e_{ij}\Psi^m(\zeta)\,\mathrm{d}\zeta, \qquad i = 1, 2, \qquad j = 4, 5$$

and $[G^{mn}]$ are the laminate matrices of electric permittivity,

$$G^{mn}_{ii} = g^0_{11}g^0_{22} \sum_{L} \int_{\zeta}^{\zeta_{+1}} \varepsilon_{ii}\Psi^m(\zeta)\Psi^n(\zeta)\,\mathrm{d}\zeta, \qquad i = 1, 2$$
$$G^{mn}_{33} = g^0_{11}g^0_{22} \sum_{L} \int_{\zeta}^{\zeta_{+1}} \varepsilon_{33}\Psi^m_{,\zeta}(\zeta)\Psi^n_{,\zeta}(\zeta)\,\mathrm{d}\zeta \tag{16}$$

and L is the number of plies in the laminate. All remaining matrix terms not shown earlier are zero.

Combining Eqs. (3) and (12) and integrating through the thickness, we find that the kinetic energy of the laminate takes the form

$$\delta T_L = \delta u_i^0 \rho_i^A \dot{u}_i^0 + \delta u_j^0 \rho_j^B \dot{\beta}_j + \delta\beta_j \rho_j^B \dot{u}_j + \delta\beta_j \rho_j^D \dot{\beta}_J \qquad i = 1, \ldots, 3, \quad j = 1, 2 \tag{17}$$

where $u_i^0 = \{u^0, v^0, w^0\}$ and $\beta_i = \{\beta_\xi, \beta_\eta\}$; ρ^A, ρ^B, and ρ^D are the generalized densities, expressing the mass, mass coupling, and rotational inertia per unit area, respectively, of the laminate,

$$\langle \rho^A, \rho^B, \rho^D \rangle = g^0_{11}g^0_{22} \sum_{L} \int_{\zeta}^{\zeta_{+1}} \rho\langle 1, \zeta, \zeta^2 \rangle \mathrm{d}\zeta \tag{18}$$

III. Finite Element Formulation

The preceding formulation of governing equations in the orthogonal curvilinear system and the attained generalized variational statement in Eq. (11) enable the development of structural solutions by using approximations of the generalized electromechanical state (displacements, rotation angles, and electric potential) on the reference surface A_0, of the following type:

$$u_j^0(\xi, \eta, t) = \sum_{i=1}^{M} u_j^{0i}(t) N^i(\xi, \eta), \qquad j = 1, \ldots, 3$$

$$\beta_j(\xi, \eta, t) = \sum_{i=1}^{M} \beta_j^i(t) N^i(\xi, \eta), \qquad j = 1, 2 \tag{19}$$

$$\phi^m(\xi, \eta, t) = \sum_{i=1}^{M} \phi^{mi}(t) N^i(\xi, \eta), \qquad m = 1, \ldots, N$$

where superscript i indicates the reference surface displacement, rotation angle, and generalized electric potential components corresponding to the ith in-plane interpolation function $N^i(\xi, \eta)$. For structural problems with general boundary, geometry, and material configurations, local interpolation functions may be used in Eqs. (19) to develop finite element based solutions. When we combine Eqs. (6), (7), (9), and (19), the strain and electric field interpolation matrices result. Substituting into the generalized equation of motion (11) and collecting the coefficients as mandated by Eqs. (13)

and (17), we find that the governing dynamic equations of the structure are expressed in a discrete matrix form,

$$\begin{bmatrix} [M_{uu}] & 0 \\ 0 & 0 \end{bmatrix} \begin{Bmatrix} \{\ddot{u}\} \\ \{\ddot{\phi}^F\} \end{Bmatrix} + \begin{bmatrix} [K_{uu}] & [K_{u\phi}^{FF}] \\ [K_{\phi u}^{FF}] & [K_{\phi\phi}^{FF}] \end{bmatrix} \begin{Bmatrix} \{u\} \\ \{\phi^F\} \end{Bmatrix} = \begin{Bmatrix} \{F(t)\} - [K_{u\phi}^{FA}]\{\phi^A\} \\ \{Q^F(t)\} - [K_{\phi\phi}^{FA}]\{\phi^A\} \end{Bmatrix} \tag{20}$$

Submatrices K_{uu}, $K_{u\phi}$, and $K_{\phi\phi}$ indicate the elastic, piezoelectric, and permittivity matrices, and M_{uu} is the mass matrix; superscripts F and A indicate the partitioned submatrices in accordance with the sensory (free) and active (applied) electric potential components, respectively. The left-hand side includes the unknown electromechanical response of the structure $\{u, \phi^F\}$, that is, the resultant displacements and voltage at the sensors. The right-hand side includes the excitation of the structure in terms of mechanical loads and applied voltages ϕ^A on the actuators. The electric charge at the sensors $Q^F(t)$ remains constant with time (practically open-circuit conditions) and is assumed to be known. Based on the preceding formulation, an eight-node ($M = 8$) finite element was developed with biquadratic shape functions of the serendipity family. The preceding dynamic system may be solved to obtain either the electrostatic response of the structure, or the modal characteristics (free vibration), or the dynamic response of the piezoelectric shell.

IV. Numerical Results and Discussion

Evaluations of the developed mechanics and applications on various composite structures with piezoceramic (PZT-4) actuators and sensors are presented. To show the location of piezoelectric layers through the thickness, the standard laminate notation is expanded such that piezoelectric layers are indicated with the letter p. The properties of all materials are provided in Table 1. The structural configurations that were studied included plates, closed cylindrical rings, simply supported cylindrical panels, and cantilever cylindrical laminated shells of various curvatures.

[p/0/90/0/p] Plate

Convergence studies and comparisons were performed with results previously obtained via exact solutions[16] and discrete-layer plate finite elements[15] for the free-vibration response of a simply supported [p/0/90/0/p] cross-ply graphite/epoxy composite plate with surface attached piezoceramic (PZT-4) layers. Because of space limitations, these studies are only summarized, and detailed descriptions are given in Ref. 28. Open (O) and closed (C) circuit conditions at piezoceramic layers were modeled to quantify the effect of piezoelectric coupling because uncoupled approaches cannot model open-circuit conditions. Excellent convergence and agreement with the exact solution were obtained for the fundamental frequency and the through-the-thickness electromechanical mode of moderately thin plates ($a/h = 50$).

Table 1 Mechanical properties ($\varepsilon_0 = 8.85 \times 10^{-12}$ F/m, electric permittivity of air)

	Graphite/epoxy	PZT-4
Elastic properties		
E_{11}, GPa	132.4	81.3
E_{22}, GPa	10.8	81.3
E_{33}, GPa	10.8	64.5
G_{23}, GPa	3.6	25.6
G_{13}, GPa	5.6	25.6
G_{12}, GPa	5.6	30.6
ν_{12}	0.24	0.33
ν_{13}	0.24	0.43
ν_{23}	0.49	0.43
Piezoelectric coefficients, 10^{-12} m/V		
d_{31}	0	−122
d_{32}	0	−122
d_{24}	0	495
d_{15}	0	495
Electric permittivity		
$\varepsilon_{11}/\varepsilon_0$	3.5	1475
$\varepsilon_{22}/\varepsilon_0$	3.0	1475
$\varepsilon_{33}/\varepsilon_0$	3.0	1300
Mass density ρ, kg/m^3	1578	7600

Closed Cylindrical Shell

The quasistatic and free-vibration response of an unsupported closed cylindrical titanium shell with a continuous piezoceramic layer on the outer surface [Ti/p] was predicted. Two types of loading conditions were examined to investigate the active and sensory response, respectively: 1) application of a sinusoidal electric potential on the outer surface of the piezoelectric layer and 2) application of a line force with free electric potential on the outer piezoelectric surface. Very good convergence was obtained in all cases for various mesh densities along the ξ and η axes, as well as very good agreement with numerical results calculated with a recently developed layerwise finite element for laminated piezoelectric solids,[24] which validate the accuracy of the present method. It was also found that the applied sinusoidal electric potential can produce significant ovalization of the active shell. More detailed descriptions of these numerical studies can be found in Ref. 28.

[0/90]$_s$ Cylindrical Panel with Continuous Actuator

The active response of a [0/90]$_s$ simply supported 90-deg cylindrical panel with a continuous PZT-4 actuator embedded at various thickness locations was modeled with a uniform 15×4 mesh along the ξ and η axes, respectively. Each graphite/epoxy ply was 0.375 mm thick, and the thickness of the PZT-4 actuator was 0.5 mm, such that the total thickness h was always 2 mm. The midsurface radius of the panel was $R/h = 100$, and the axial-to-hoop-length ratio $L_\eta/L_\xi = 1$. Three different laminate configurations were considered, representing placement of the actuator at the outer surface ([0/90$_2$/0/p]), middle surface ([0/90/p/90/0]), and inner surface ([p/0/90$_2$/0]) of the panel, respectively. The actively induced radial deflections along the axial midspan ($L_\eta/2$) of the panel are shown in Fig. 3, with a uniform electric field of $E_3(\xi, \eta) = \pm 400$ kV/m applied on the actuator. Figure 3 shows that the thickness placement of actuators has a significant and complicated effect on the response of this active panel. Results from a Ritz solution using the MSPT and utilizing trigonometric in-plane global functions in Eq. (19) are also shown in Fig. 3. The finite element predictions have exactly duplicated the Ritz solution, indicating the excellent convergence of the element.

Cantilever Cylindrical Shells

The remaining case studies illustrate the response of cantilever graphite/epoxy cylindrical shells with either a continuous PZT-4 layer or four curved patches attached on each side of the composite shell, covering 80% of the free area. The thickness of each composite ply is 0.12 mm, whereas the thickness of each piezoelectric layer is 0.24 mm. The circumferential length $L_\xi = 0.314$ m and the aspect ratio $L_\xi/L_\eta = 5$ remains constant. The midsurface radius was varied to study the effects of curvature of the active/sensory response of the shell. The shell configuration, the curvilinear coordinate system, and the finite element discretization are shown in Fig. 4 for a semicircular shell. Three discrete layers ($N = 4$) were used for the electric

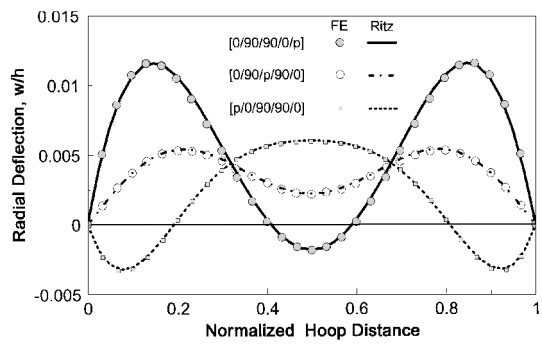

Fig. 3 Effect of through-the-thickness actuator placement on a simply supported quarter-circular [0/90]$_s$ cylindrical panel; uniform electric field $E_3(\xi, \eta) = \pm 400$ kV/m applied.

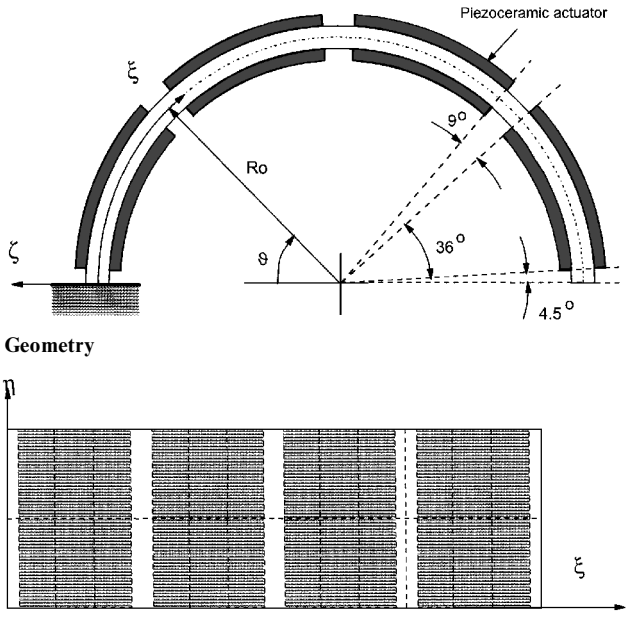

Fig. 4 Semicircular cantilever shell with eight surface-bonded cylindrical piezoceramic patches.

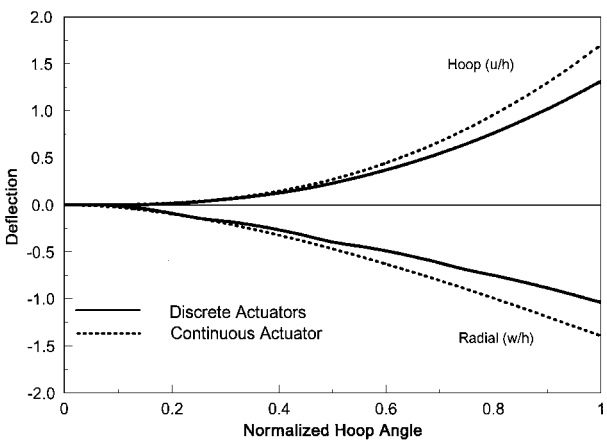

Fig. 5 Active radial and circumferencial deflections of the semicircular [45/−45/0]$_s$ cantilever shell; 100 V applied on each piezoelectric layer.

potential field, one for each piezoelectric layer and one for the composite laminate. In all cases, the electric potential at the bonded surface of the piezoelectric patches was forced to remain zero. The specification of the other two generalized electric potential values results in various active and/or sensory configurations of the smart shell.

Active Case

The active radial (w^0) and hoop (u^0) deflections for a semicircular [p/45/−45/0]$_s$ shell are shown in Fig. 5, with 100 V applied on the free surface of each piezoceramic. For comparison purposes, Fig. 5 shows the active deflections of the shell induced either by the eight curved piezoceramic patches or by two continuous piezoceramic layers of same thickness attached at the inner and outer surface. The effect of discrete actuators on the deflected shape of the shell is obvious and can be attributed to the nonuniform actuation and laminate stiffness resulting from the discrete actuators. It is important to point out the relatively high radial and hoop deflections at the free end. This highlights the possibility to achieve substantially large, yet accurate, and rapid free-end positioning with such active cantilever shells.

The effect of curvature, expressed by the ratio h/R, on the active tip deflection of the shell is shown in Fig. 6 for the case of two continuous actuators. The results clearly illustrate that active cantilever cylindrical shells have the potential to achieve two-dimensional positioning of their free end, as opposed to the case of the cantilever plate ($h/R = 0$), which undergoes only transverse deflections.

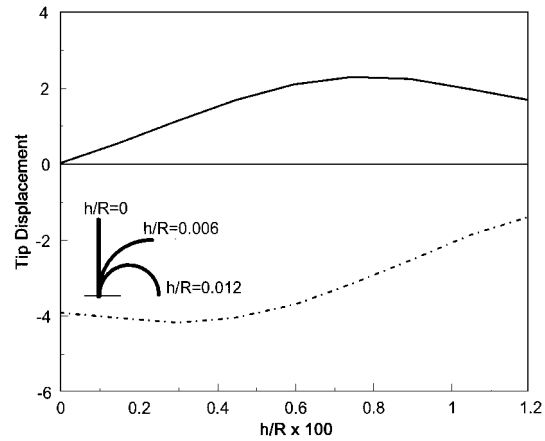

Fig. 6 Effect of curvature on the tip displacement of a [p_2/45/−45/0]$_s$ cantilever shell with continuous actuators; 100 V applied on each piezoelectric layer: ——, hoop (u/h) and – ‗–, radial (w/h).

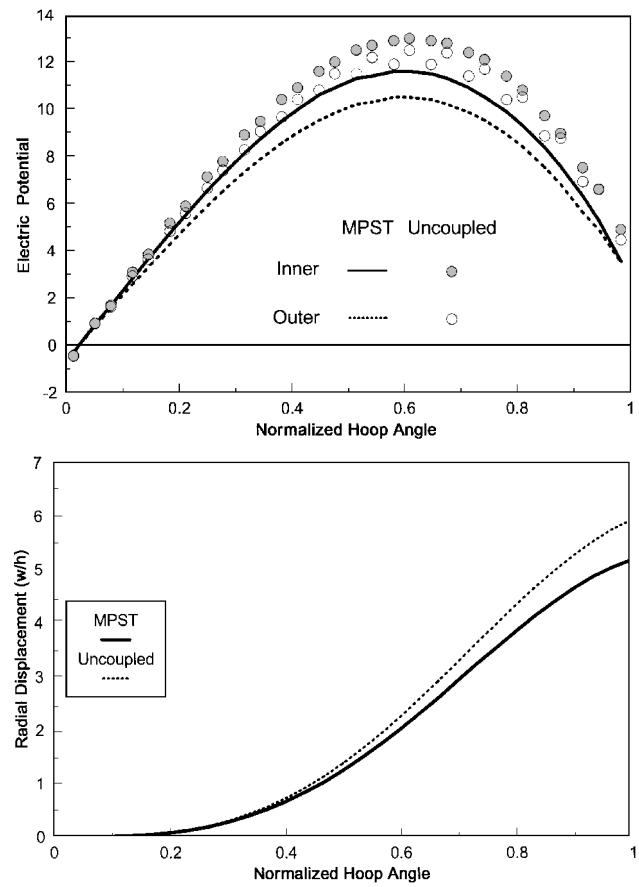

Fig. 7 Sensory electric potential ($\phi d_{31}/h \times 10^6$) and radial deflection predictions of a semicircular [p_2/0/90/45/−45]$_s$ cantilever shell with continuous piezoelectric sensors; radial line load $F_\zeta = 159.2$ N/m is applied at the free end.

Higher active tip deflections may also be achieved within certain curvature ranges, thus increasing the effectiveness of piezoelectric actuators. These beneficial effects can be attributed to the capability of curved actuators to simultaneously actuate both in-plane and transverse displacements [see Eq. (6)].

Sensory Case

The response of a [p/0/90/$\pm$45]$_s$ cantilever shell with all piezoelectric layers configured as sensors (free electric potential) was also modeled. In all cases, a radial line load in the hoop direction $F_\zeta = 159.2$ N/m was applied at the free end, and the electric potential was normalized as $\phi d_{31}/h \times 10^6$. Figure 7 shows the radial deflection and the sensory electric potential of a semicircular shell with continuous piezoelectric sensors. The differences in the predictions

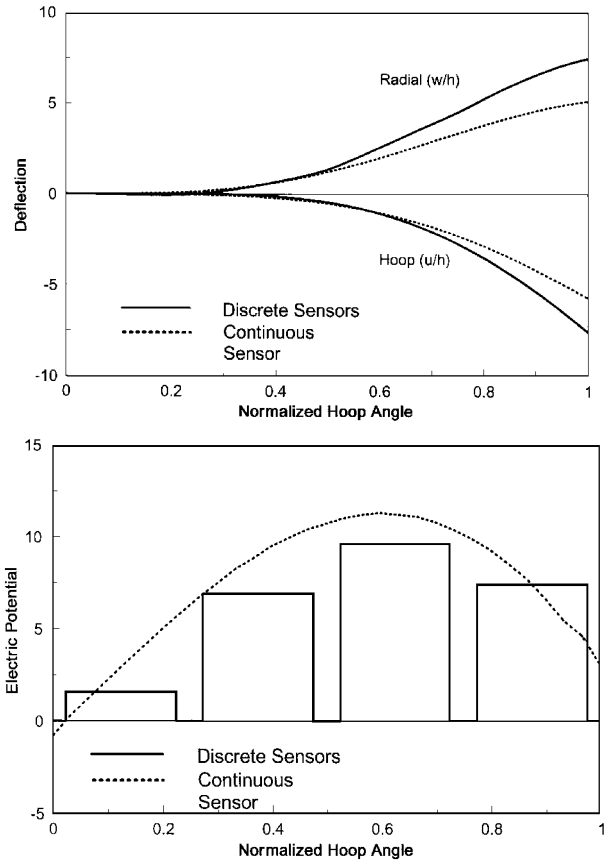

Fig. 8 Radial and circumferencial deflections and corresponding sensory electric potential ($\phi d_{31}/h \times 10^6$) of the semicircular [p_2/0/90/45/ _45]$_s$ cantilever shell with discrete sensors; radial line load $F_\zeta = 159.2$ N/m is applied along the free end.

of the present theory (MPST) vs an uncoupled approach, which neglects the piezoelectric coupling mandated by Eqs. (2) and (13), are also compared in Fig. 7. The sensory electric potential values of the uncoupled theory were recovered from the generalized strains at the integration points, using the equation of charge conservation for thin shells,[22] whereas the electric potential predictions of MPST at the respective integration points were interpolated from nodal values using the third equation of Eq. (19). Selective reduced integration was used in this case to reduce oscillations in the sensory voltage observed with the uncoupled approach. Clearly, uncoupled approaches overestimate the deflection and sensory voltage. Moreover, Fig. 7 indicates the suitability of the MPST to provide piecewise continuous and stable sensory voltages with finite element discretization, as opposed to the uncoupled approaches that effectively provide only sensory voltages at integration points of inferior numerical quality.

Figure 8 shows the difference between continuous sensors and the more realistic case of eight curved piezoceramic patches (Fig. 4) with continuous electrodes on their free surface. A continuous surface electrode forces a uniform electric potential over the surface, which was represented with equality constraints on the electric potential. The resultant displacements and corresponding voltages at each sensor are shown in Fig. 8, respectively. The presence of discrete piezoelectric sensors has a definite effect on the deflected shape, as well as the sensory voltage values. Figure 8 also illustrates that the response of discrete sensors may be only roughly approximated with the consideration of a continuous layer. Hence, many proposed methods attempting to replicate discrete sensors by averaging electric potential over segments of a continuous piezoelectric layer may lead to considerable error.

The effect of curvature on the sensory voltage of the cantilever shell with continuous piezoelectric layers is shown in Fig. 9 for a semicircular and quarter-circular shell vs a cantilever plate, all having identical length $L_\xi = 0.314$ m and aspect ratio $L_\xi / L_\eta = 5$. The cantilever plate exhibits monotonic and identical sensory voltages at

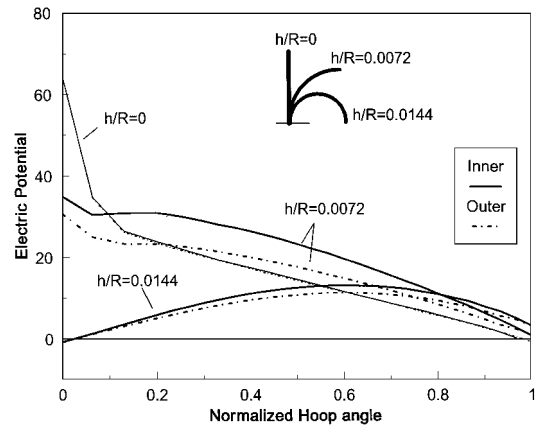

Fig. 9 Effect of curvature on the sensory electric potential ($\phi d_{31}/h \times 10^6$) of a cylindrical [p_2/0/90/45/_45]$_s$ cantilever shell with continuous piezoelectric sensors; radial line load F_ζ = 159.2 N/m is applied at the free end.

two piezoelectric layers, whereas the introduction of constant curvature results in notable changes in the voltage variations, thus making the relation between deformed shape and sensory voltage less apparent. Moreover, Fig. 9 also shows different sensory voltages in the inner and outer piezoelectric layer of the curved shells, respectively, which is attributed to through-the-thickness strain asymmetry introduced by curvature. Consequently, the results indicate that the through-the-thickness placement of the piezoelectric sensor may affect its sensory voltage output in smart piezoelectric shells.

V. Summary

Mechanics for the analysis of laminated composite shells with piezoelectric actuators and sensors were presented. The mechanics were based on a new mixed-field theory for curvilinear laminates that combines single-layer assumptions for the displacements with a layerwise representation of the electric potential. The resulting governing coupled equations for piezoelectric shell laminates and structures were developed in curvilinear coordinates. Based on them, finite element based analysis procedures for piezoelectric composite shell structures were described, and an eight-node shell finite element was formulated for the static and dynamic analysis of composite shells containing piezoelectric actuators and sensors. The described mechanics, the finite element, and the computational procedure were encoded in prototype software.

Evaluations and excellent comparisons were obtained with reported results for thin piezoelectric composite plates and shells. Applications of the method on the analysis of simply supported cylindrical shells with an active piezoelectric layer were performed, illustrating the effect of through-the-thickness actuator placement on the deformed shape of the shell. The active and sensory response of laminated cantilever cylindrical shells with continuous piezoceramic layers or discrete curved piezoceramic patches was also analyzed, and the effects of curvature on the active and sensory response were quantified. Overall, the numerical results have demonstrated the accuracy, versatility, and advantages of the present formulation for analyzing the response of thin and intermediately thick piezoelectric-composite shell structures.

Acknowledgments

This work was supported by NASA Cooperative Agreement NCC3-391. Dale A. Hopkins was the Project Manager. This support is gratefully acknowledged.

References

[1]Lee, C. K., and Moon, F. C., "Laminated Piezopolymer Plates for Torsion and Bending Sensors and Actuators," *Journal of the Acoustical Society of America*, Vol. 85, No. 6, 1989, pp. 2432–2439.

[2]Lee, C. K., "Theory of Laminated Piezoelectric Plates for the Design of Distributed Sensors/Actuators. Part I: Governing Equations and Reciprocal Relationships," *Journal of the Acoustical Society of America*, Vol. 87, No. 3, 1990, pp. 1144–1158.

[3]Lee, C. K., and Moon, F. C., "Modal Sensors/Actuators," *Journal of Applied Mechanics*, Vol. 57, June 1990, pp. 434–441.

[4]Wang, B. T., and Rogers, C. A., "Laminate Plate Theory for Spatially Distributed Induced Strain Actuators," *Journal of Composite Materials*, Vol. 25, No. 4, 1991, pp. 433–452.

[5]Crawley, E. F., and Lazarus, K. B., "Induced Strain Actuation of Isotropic and Anisotropic Plates," *AIAA Journal*, Vol. 29, No. 6, 1991, pp. 944–951.

[6]Allik, H., and Hughes, T. J. R., "Finite Element for Piezoelectric Vibration," *International Journal for Numerical Methods in Engineering*, Vol. 2, No. 2, 1970, pp. 151–157.

[7]Naillon, M., Coursant, R. H., and Besnier, F., "Analysis of Piezoelectric Structures by a Finite Element Method," *Acta Electronica*, Vol. 25, No. 4, 1983, pp. 341–362.

[8]Tzou, H. S., and Tseng, C. I., "Distributed Piezoelectric Sensor/Actuator Design for Dynamic Measurement/Control of Distributed Parametric Systems: A Piezoelectric Finite Element Approach," *Journal of Sound and Vibration*, Vol. 138, No. 1, 1990, pp. 17–34.

[9]Ha, S. K., Keilers, C., and Chang, F. K., "Finite Element Analysis of Composite Structures Containing Distributed Piezoceramic Sensors and Actuators," *AIAA Journal*, Vol. 30, No. 3, 1992, pp. 772–780.

[10]Pauley, K. P., "Analysis of Plane Waves in Infinite, Laminated, Piezoelectric Plates," Ph.D. Dissertation, Dept. of Engineering Mechanics, Univ. of California, Los Angeles, CA, 1974.

[11]Robbins, D. H., and Reddy, J. N., "Analysis of Piezoelectrically Actuated Beams Using a Layer-Wise Displacement Theory," *Computers and Structures*, Vol. 41, No. 2, 1991, pp. 265–279.

[12]Robbins, D. H., and Reddy, J. N., "Modelling of Thick Composites Using a Layerwise Laminate Theory," *International Journal for Numerical Methods in Engineering*, Vol. 36, No. 4, 1993, pp. 655–677.

[13]Heyliger, P. R., Ramirez, G., and Saravanos, D. A., "Coupled Discrete-Layer Finite Elements for Laminated Piezoelectric Plates," *Communications in Numerical Methods in Engineering*, Vol. 10, 1994, pp. 971–981.

[14]Saravanos, D. A., and Heyliger, P. R., "Coupled Layerwise Analysis of Composite Beams with Embedded Piezoelectric Sensors and Actuators," *Journal of Intelligent Material Systems and Structures*, Vol. 6, No. 3, 1995, pp. 350–363.

[15]Saravanos, D. A., Heyliger, P. R., and Hopkins, D. A., "Layerwise Mechanics and Finite Element for the Dynamic Analysis of Piezoelectric Composite Plates," *International Journal of Solids and Structures*, Vol. 34, No. 3, 1997, pp. 359–378.

[16]Heyliger, P. R., and Saravanos, D. A., "Exact Free-Vibration Analysis of Laminated Plates with Embedded Piezoelectric Layers," *Journal of the Acoustical Society of America*, Vol. 98, No. 3, 1995, pp. 1547–1557.

[17]Dökmeci, C. M., "Shell Theory for Vibrations in Piezoceramics Under a Bias," *IEEE Transactions on Ultrasonics, Ferroelectrics, and Frequency Control*, Vol. 37, No. 5, 1990, pp. 369–385.

[18]Lammering, R., "The Application of a Finite Shell Element for Composites Containing Piezoelectric Polymers in Vibration Control," *Computers and Structures*, Vol. 41, No. 5, 1991, pp. 1101–1109.

[19]Koconis, D. B., Kollar, L. P., and Springer, G. S., "Shape Control of Composite Plates and Shells with Embedded Actuators. I. Voltages Specified," *Journal of Composite Materials*, Vol. 28, No. 5, 1994, pp. 415–458.

[20]Tzou, H. S., and Garde, M., "Theoretical Analysis of a Multi-Layered Thin Shell Coupled with Piezoelectric Shell Actuators for Distributed Vibration Controls," *Journal of Sound and Vibration*, Vol. 132, No. 3, 1989, pp. 433–450.

[21]Larson, P. H., and Vinson, J. R., "The Use of Piezoelectric Materials in Curved Beams and Rings," *Adaptive Structures and Material Systems*, edited by G. P. Carman and E. Garcia, AD-Vol. 35, Winter Annual Meeting, American Society of Mechanical Engineers, New York, 1993, pp. 277–285.

[22]Tzou, H. S., and Zhong, J. P., "Electromechanics and Vibrations of Piezoelectric Shell Distributed Systems," *Journal of Dynamic Systems, Measurement and Control*, Vol. 115, Sept. 1993, pp. 506–517.

[23]Tzou, H. S., and Ye, R., "Analysis of Piezoelastic Structures with Laminated Piezoelectric Triangle Shell Elements," *AIAA Journal*, Vol. 34, No. 1, 1996, pp. 110–115.

[24]Heyliger, P. R., Pei, K. C., and Saravanos, D. A., "Layerwise Mechanics and Finite Element Model for Laminated Piezoelectric Shells," *AIAA Journal* (to be published).

[25]Tiersten, H. F., *Linear Piezoelectric Plate Vibrations*, Plenum, New York, 1969.

[26]Fung, Y. C., *Foundations of Solid Mechanics*, Prentice–Hall, Englewood Cliffs, NJ, 1965.

[27]Soedel, W., *Deep Shell Equations, Vibrations of Shells and Plates*, Marcel Dekker, New York, 1993.

[28]Saravanos, D. A., "Coupled Mixed-Field Laminate Theory and Finite Element for Smart Piezoelectric Composite Shell Structures," NASA CR 198490, 1996.

R. K. Kapania
Associate Editor